

UNIVERSITY OF PÉCS

Biological Doctoral School

**Characterization of the Vestibular NADPH Oxidase
Enzyme Complex**

PhD thesis

PÉTER KISS

Thesis supervisors:

Dr. Joseph Zabner MD

Dr. Kerepesi Ildikó, PhD

Pécs, 2009

INTRODUCTION

NADPH oxidases

All aerobic organisms are exposed to reactive oxygen species (ROS), such as hydrogen peroxide (H_2O_2), the superoxide anion (O_2^-) and the hydroxyl radical (OH_2), as by-products of oxidative metabolism and through exposure to radical-generating compounds. Enhanced oxidative stress has been implicated in the pathogenesis of several clinical disorders, such as heart and brain ischemic diseases, neurodegenerative disorders, and various autoimmune diseases, and it seems to be involved in carcinogenesis and aging as well as in anti-microbial host defense.

Several enzymes evolved for ROS production belong to the recently discovered NADPH oxidase (NOX) enzyme family, which consists of 7 members in human: NOX1- 5, and the dual oxidases (DUOX1, 2). These enzymes share the capacity to transport electrons across a biological membrane and to generate superoxide and/or hydrogen peroxide.

The phagocytic NADPH oxidase (NOX2) is a well-known enzyme complex that plays a critical role in antimicrobial host defenses, which requires several regulatory subunits for its function including an activator ($p67^{phox}$) and an organizer protein ($p47^{phox}$). The close homology between NOX1, which utilizes the $p47^{phox}$ and $p67^{phox}$ homologues NOXO1 and Noxa1 for its function, NOX2 and NOX3 suggests that NOX3 may also require regulatory subunits for its function. NOX3 is highly expressed in the inner ear. Characterization of the “head tilt” mutant mouse, which has vestibular defects, established a functional role of NOX3 in the inner ear. *In vitro*, NOX3 activity is also enhanced in the presence of $p47^{phox}$ and $p67^{phox}$, NOXO1 and NOXA1. However, the physiologically relevant partners of NOX3 have not been defined.

The anatomy of the vestibule

The vestibule, part of the vestibular system, is the sensory organ that provides the dominant input about our movement and orientation in space. As our movements consist of rotations and translations, the vestibule comprises two components: the three semicircular canals, which are sensitive to angular acceleration, and the vestibular sacs, which detect linear acceleration and gravity. The portion of the vestibular apparatus which is responsible for the detection of directional (positional) movement (i.e. tilting of head) consists of two flattened, spot-like areas (maculae) located in the saccular and utricular cavities of the membranous labyrinth. In transverse section, the macula utriculi and macula sacculi are both organized into a single layer of cells consisting of supportive cells residing on a basement membrane and two types of sensory hair cells. The vestibular system of the inner ear continuously informs the brain about the accelerations and the position of the head. Detection of gravity requires special structures, called otoconia, with large inert mass and some mobility. In the absence of otoconia, the otolith organs “mislead” the brain by continuously conveying the signal of freefall independently from the movements of the head. The biological mechanisms responsible for development, biosynthesis, and maintenance of otoconia are not completely understood.

AIMS OF THE STUDY

The main goals of the present study were:

1. Identify and characterize *Noxo1* mutant mouse strains.
2. We sought to determine the biological importance of *Noxo1*.
3. *In vivo* characterization of the vestibular NADPH oxidase 3 (Nox3) complex.
4. Generation of *Noxa1* KO mouse model in order to determine its role in the inner ear.
5. Identification and characterization of a p22^{phox} deficient mouse strain.

METHODS

Mouse lines and genotyping

Wild type mice (SJL.Thy1^a) and the 'head slant' (*hslt*) balance deficient mutant strain were obtained from Jackson Laboratory. Genomic DNA of a heterozygous *hslt* mouse was prepared from tail snips using proteinase K digestion followed by phenol-chloroform extraction. The one nucleotide difference between the *Noxo1*^{wt} and *Noxo1*^{hslt} alleles was detected by sequencing analysis and by PCR using HotStart Taq DNA polymerase capitalizing on the importance of a perfect match for the 3' end of the PCR primers. The following PCR cycle was used for genotyping: for *Noxo1*^{wt}: Initial Denaturation Step 95°C for 15 min, Denaturation Step 94°C for 30 sec, Primer Annealing Step 73°C for 30 sec, Extending Step 73°C for 30 sec, Number of Cycles 36, Final Extending Step 73°C for 10 min, product size 248bp, for *Noxo1*^{hslt}: initial Denaturation Step 95°C for 15 min, Denaturation Step 94°C for 30 sec, Primer Annealing Step 71°C for 30 sec, Extending Step 72°C for 30 sec, Number of Cycles 36, Final Extending Step 72°C for 10 min, product size 368bp and for *Noxo1*^{transgenic}: initial Denaturation Step 95°C for 15 min, Denaturation Step 94°C for 30 sec, Primer Annealing Step 65°C for 30 sec, Extending Step 72°C for 1min and 20 sec, Number of Cycles 38, Final Extending Step 72°C for 10 min, product size 1331bp. For swim test, wild type (*n*=21) and homozygous *hslt* (*n*=21) mice were placed into room temperature tap water for 30 and 7 s, respectively.

Conventional and real-time RT-PCR

Total RNA was isolated with Trizol reagent or with RNeasy Mini Kit. The integrity of the total RNA was checked by denaturing formaldehyde agarose gel electrophoresis and the quantity was assessed by UV spectrophotometry. The total RNA samples were DNase I treated, reverse transcribed by SuperScript II, and used in PCR experiments. For Quantitative Real-time PCR, total RNA was extracted from homogenized tissues using Trizol reagent, then DNase I treated, further purified using RNeasy kit, and reverse-transcribed by Thermoscript reverse transcriptase. Real-time PCR was performed with primers specific for the gene of interests and the

control 18S transcripts. The amounts of PCR products were measured using SYBR Green and ABI PRISM 7700 Sequence Detection System.

Generation of *Noxo1* transgenic mice

The cDNA encoding *Noxo1* was subcloned into pSTEC-1 vector under the control of different promoters (CMV, CBA, or putative endogenous *Noxo1*). The pSTEC-1 construct also contained a chimeric intron and an SV40 polyadenylation site required for proper processing of the transgene mRNA *in vivo*. The entire *Noxo1* expression cassette was isolated by restriction digestion (*KpnI*) followed by gel extraction and used for microinjection into pronuclei of fertilized oocytes (C57BL/6 X SJL.F2), which were transferred into pseudopregnant foster mothers. The presence of the *Noxo1* transgene was determined by PCR using standard reaction conditions. Transgenic mice were bred with *Noxo1*^{hslt}/*Noxo1*^{hslt} animals for two consecutive generations to obtain *Noxo1*^{hslt}/*Noxo1*^{hslt} and transgene positive genotype.

Histology, immunohistochemistry, and microscopy

Inner ears of *hslt*, wild type, and *Noxo1* transgene rescued *hslt* mice embryonic day 17 and postnatal day 0-2 (ED17 and P0-2) were fixed in 4% PBS-buffered paraformaldehyde, paraffin embedded, sectioned (10 μm), and deparaffinized.

The slides were then used for von Kossa staining, OC-90/95 immunohistochemistry using two different rabbit polyclonal antibodies. For scanning electron microscopy, mouse heads (P1) were fixed in 4% PBS-buffered paraformaldehyde and embedded into paraffin. After preparing coronal sections, tissue blocks were deparaffinized and fixed in 4% osmium tetroxide in distilled water. Samples were dehydrated, critical-point-dried in CO₂, coated with gold-palladium, and examined using a Hitachi S4000 scanning electron microscope at 5 kV. For transmission electron microscopy the temporal bones of mouse heads were removed and fixed in Karnovsky's fixative, postfixed for 2h in 1% OsO₄, dehydrated in graded alcohol and acetone, and embedded into Spurr's resin. Thin sections (150 nm) were cut and stained with uranyl acetate and lead citrate, and then examined with JEOL JEM-1230 Transmission Electron Microscope. For X-ray photoelectron spectroscopy mouse heads were frozen in Tissue-Tek O.C.T. Compound, then cryosectioned until the

plane of sacculae was reached. All XPS measurements were performed using Kratos Axis Ultra XPS spectrometer with the base pressure of $\sim 5 \times 10^{-9}$ Torr. All spectra were analyzed using the CasaXPS software (CasaXPS Version 2.3.10, 1999-2005). XPS data fitting was performed using Shirley background subtraction.

In situ hybridization

Mouse heads (ED17 and P0) were fixed in 4% PBS-buffered paraformaldehyde, and 10 μm thick coronal cryosections were mounted onto poly-L-lysine slides. P^{33} -labeled antisense and sense cRNA probes (nucleotide 431-630 base pair of *mNoxo1* cDNA) were generated with MAXIscript *in vitro* transcription kit (Ambion) and hybridized with the tissue sections using mRNA locator kit (Ambion) following the manufacturer's instructions. Slides were stained with hematoxylin & eosin and exposed to photosensitive emulsion. To visualize silver grains only and exclude outlines of the tissue, dark field microscopy images were taken using Kodak Wratten 31 medium magenta filters.

Cell culture, DNA constructs, transfection, and superoxide detection

HEK293T cells were maintained in Dulbecco's modified Eagle's medium, culture media were supplemented with 10% fetal calf serum, penicillin (100 units/ml), streptomycin (100 $\mu\text{g}/\text{ml}$), and 4 mmol/liter L-glutamine.

Human and mouse *Noxo1*^{hsl} mutant cDNAs were generated with PCR using internal, overlapping primers cDNAs with inserted Kozak sequences were subcloned into pcDNA3.1. To obtain stable clones, HEK293 cells were selected with 400 $\mu\text{g}/\text{ml}$ Geneticin (an aminoglycoside antibiotic G418) starting on the 2nd day after transfection, and 13 surviving colonies were isolated 10 days after the transfection.

ROS generation was measured, by the peroxidase-dependent luminol-amplified chemiluminescence technique on a Luminometer Wallac 1420 Multilabel Counter (PerkinElmer Life Sciences). Superoxide production cells were plated into 96/48-well microplates and superoxide production was measured following SOD-dependent reduction of 100 μM ferricytochrome c at 550 nm in Hanks' balanced salt solution, or Hanks' balanced salt solution supplemented with 6 units/ml horseradish peroxidase and 250 μM luminol.

Generation of *Noxa1* knockout mouse model

RPCI - 21 Female (129S6/SvEvTac) Mouse PAC Library was screened for *Noxa1* gene by hybridization of *Noxa1* probe on high density filter. PAC vector RP21-96I18 was identified as containing mouse *Noxa1* gene and was used for the amplification of the left (2331bp) and right arm (3551bp) of the targeting vector. The arms were cloned into pRAY-2 cloning vector.

A targeting vector designed to replace exons II–VI of the *Noxa1* gene was constructed. For the generation of *Noxa1*-deficient mice, 129SvJ embryonic stem cells were electroporated with *NotI* linearized targeting vector construct (9954bp). G418 resistant clones were analysed by PCR screen and verified by Southern blot.

p22^{phox} transgenic mouse strain

The CBA promoter region was subcloned into pSTEC-1 vector. p22^{phox} cDNA was subcloned 3' from the promoter and 5' from an SV40 polyA signal. The expression cassette (1907bp) was isolated by *KpnI* restriction enzyme and microinjected into pronuclei of fertilized oocytes (C57BL/6 X SJL.F2) that were transferred into pseudopregnant foster mothers. The presence of the transgene was determined by PCR using Taq DNA polymerase. Transgene positive mice were bred with homozygote *nmf333* mice for two consecutive generations to obtain *nmf333/nmf333* and transgene positive genotype.

Nitroblue Tetrazolium test (NBT)

Blood was taken from the tail vein of either wt or *nmf333* mutant mice. Blood cells were seeded onto microscopic slide in the presence or absence of 10µg/ml PMA (phorbol 12-myristate 13-acetate) and incubated for 45 minutes at 37°C. After gently washed with PBS, cells were incubated at 37°C for 15 min in Hanks' balanced salt solution containing 0.5 mg/ml nitroblue tetrazolium (NBT). After incubation, the cells were washed with PBS and fixed in 100% methanol. The percent of NBT-positive (i.e. blue-gray staining of cytoplasm) granulocytes were determined.

RESULTS AND DISCUSSION

Identification and characterization of a Noxo1 mutant mouse strain

Based on our *in vitro* results, we hypothesized that Nox3 requires NADPH oxidase organizer 1 (Noxo1) and activator 1 (Noxa1) for its function, as well as the p22^{phox} regulatory subunit. In mice, mutations in the *Nox3* gene have been shown to manifest a defect in balance. We searched databases for mice with non-syndromic vestibular deficit. We identified a ‘head slant’ (*hslt*) mouse strain with a spontaneous mutation in the *Noxo1* gene. The balance deficit of homozygous mice of *hslt* line was manifested as early as day 4 after birth. Pups that were placed on their back did not attempt to right themselves to the ventral position. From day 18, they exhibited distinct head and body tilt and an abnormal reaching response during falling compared to heterozygous littermates or in wild type mice. Unlike control mice, affected mutants could not orient themselves in water and thus became submerged and introduced a so-called “non-swimming” phenotype. Histological analysis by von Kossa staining of inner ears of embryonic day (ED) 17 and newborn (postnatal day 0-2, P0-2) *Noxo1^{hslt}/Noxo1^{hslt}* mice demonstrated the complete absence of calcium carbonate crystallization in *Noxo1^{hslt}/Noxo1^{hslt}* inner ears. Scanning electron microscopy not only verified the lack of otoconia in *Noxo1^{hslt}/Noxo1^{hslt}* animals but also showed coral-like conglomerates above the hair cells. Immunohistological analysis has shown that the conglomerates are composed of OC-90/95 protein and may preserve a brief developmental stage prior to calcium carbonate mineralization.

The biological importance of Noxo1

In order to demonstrate that the severe imbalance of *hslt* mice was caused by the mutation in *Noxo1*, and not in a linked gene, we used transgenic rescue. We generated mice containing CMV promoter-driven *Noxo1* transgene. Mice were bred with *Noxo1^{hslt}/Noxo1^{hslt}* mice for two consecutive backcross generations to obtain transgene positive *Noxo1^{hslt}/Noxo1^{hslt}* mice.

Fourteen transgene positive *Noxo1^{hslt}/Noxo1^{hslt}* animals have been identified with wild type phenotype including their ability to swim and by von Kossa staining showing restored otoconia suggesting that expression of the transgene rescued defects in the *Noxo1^{hslt}/Noxo1^{hslt}* mice and formally proving that the mutation in *Noxo1* was indeed responsible for the balance deficit of the *hslt* line.

***In vivo* characterization of the vestibular NADPH oxidase 3 (Nox3) complex**

We investigated whether the *hslt* mutation of Noxo1 may prevent ROS production by a Nox3-Noxo1 containing enzyme complex. HEK293T cells were transfected with mouse Nox3, Noxo1^{wt} or Noxo1^{hslt} with or without Nox activator 1 (Noxa1). Superoxide production was measured by the superoxide dismutase-dependent reduction of ferricytochrome c. We chose Noxa1 as the potential activator subunit of Nox3, since it was expressed in embryonic inner ear and the lack of the only other known Nox activator, p67^{phox}, does not cause balance problems in patients with p67^{phox}-deficient chronic granulomatous disease. Mouse Nox3 required the co-transfection of both mouse Noxo1^{wt} and Noxa1 to achieve maximal superoxide generation. Furthermore, replacement of Noxo1^{wt} by Noxo1^{hslt} drastically reduced Nox3 enzyme activity independent of combination of the subunits.

Generation of *Noxa1* KO mouse model in order to determine its role in the inner ear

In vitro studies have demonstrated that Nox3, similar to Nox1 and Nox2, is also depended on a Nox activator (e.g. Noxa1 or p67^{phox}) in transfected HEK293 cells. We hypothesized that Nox3 requires Noxa1, To test this hypothesis we generated *Noxa1* deficient mice. It was previously shown that the N-terminal half of the protein is crucial for its function, we decided to target this region. Analysis of these mice will provide a useful tool for the understanding of the function of the Nox3 and Nox1 complex which very likely utilizes Noxa1 as its activator subunit.

Identification and characterization of a p22^{phox} deficient mouse strain

Nox1 and Nox3 are not sufficient to form a ROS-producing complex in transfected cells. Thus, either p22^{phox} or another protein with functional similarities is likely a critical subunit of the vestibular NADPH oxidase. Interestingly, the phenotypic allele of a balance deficient mutant mouse line, nmf333, has been localized to the region where the p22^{phox} gene (CYBA) is found (chr. 8, ~67 cM). This phenotype is described as head- and body tilt that can be observed at approximately 4 weeks of age. We hypothesized that the nmf333 mutant mouse possesses a mutation in the mouse p22^{phox} gene, thus we ordered the nmf333 strain from Jackson Laboratories for further characterization. The sequencing results revealed that the mutation is indeed located in the p22^{phox} gene. The thymidine at position 361 was substituted with a cytosine, which resulted in tyrosine to histidine amino acid change at position 121. To determine whether the mutation also results in functional loss of the protein, we performed the well-known diagnostic nitroblue tetrazolium NBT test, which determines the functional loss of the phagocytic NADPH oxidase complex in neutrophils. The NBT test performed on blood from homozygous mice showed negative results. We generated a construct expressing the mutant protein and overexpressed it in EBV transformed B cells derived from p22^{phox} deficient patient. While the wt p22^{phox} protein expressing construct restored the phenotype of the p22^{phox} deficient B cells, the mutant protein failed to restore superoxide production. To confirm the balance deficit reported by Jackson Laboratories in these mice, we performed the swimming test that showed results similar to Nox1 deficient mice. These results suggest that p22^{phox} might be a component of the vestibular NADPH complex. To prove this, we designed a transgenic construct to overexpress p22^{phox} in nmf333 mice. If the overexpression of the transgene restores the phenotype will not only prove that p22^{phox} is an indispensable partner of Nox3 but it will also provide a useful tool to study the function of Nox1 in the colon that also likely requires p22^{phox} as a subunit for its full function.

In conclusion, this work has identified Nox1 as the organizer subunit of the vestibular NADPH oxidase system and provided evidence that p22^{phox} and possibly

NOXA1 are also part of the vestibular ROS generating enzyme complex (Figure 1). These data help our understanding about the development of the inner ear and further insights into the biological function of reactive oxygen species.

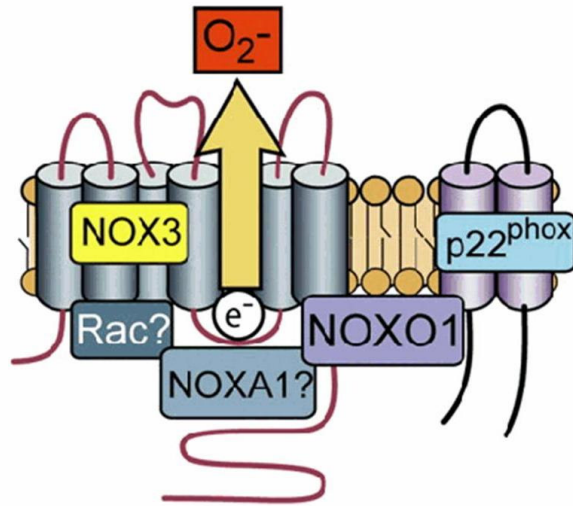


Figure 1. The vestibular NADPH oxidase enzyme complex with the known and possible subunits

PUBLICATIONS

Publications related to the thesis

Péter J. Kiss, Judit Knisz, Yuzhou Zhang, Jonas Baltrusaitis, Curt D. Sigmund, Ruediger Thalmann, Richard J.H. Smith, Elisabeth Verpy, Botond Bánfi. Inactivation of NADPH oxidase organizer 1 results in severe imbalance *Curr Biol.* 2006 Jan 24;16(2):208-13. (IF: 11.733)

Publications not related to the thesis

Stoltz DA, Ozer EA, Taft PJ, Barry M, Liu L, **Kiss PJ**, Moninger TO, Parsek MR, Zabner J. Drosophila are protected from Pseudomonas aeruginosa lethality by transgenic expression of paraoxonase-1. *J Clin Invest.* 2008 Sep 118(9):3123-31. (IF: 16.915)

Szanto I, Rubbia-Brandt L, **Kiss P**, Steger K, Banfi B, Kovari E, Herrmann F, Hadengue A, Krause KH. Expression of NOX1, a superoxide-generating NADPH oxidase, in colon cancer and inflammatory bowel disease. *J Pathol.* 2005 Oct;207(2):164-76. (IF: 6.213)

Gascon E, Vutskits L, Zhang H, Barral-Moran MJ, **Kiss PJ**, Mas C, Kiss JZ. Sequential activation of p75 and TrkB is involved in dendritic development of subventricular zone-derived neuronal progenitors in vitro. *Eur J Neurosci.* 2005 Jan;21(1):69-80 (IF: 3.949)